Nanoscale Res Lett (2008) 3:179–185
DOI 10.1007/s11671-008-9133-5

NANO EXPRESS

Deep Level Transient Spectroscopy in Quantum Dot Characterization

O. Engström · M. Kaniewska

Received: 11 March 2008 / Accepted: 5 May 2008 / Published online: 28 May 2008

Abstract Deep level transient spectroscopy (DLTS) for investigating electronic properties of self-assembled InAs/GaAs quantum dots (QDs) is described in an approach, where experimental and theoretical DLTS data are compared in a temperature-voltage representation. From such comparative studies, the main mechanisms of electron escape from QD-related levels in tunneling and more complex thermal processes are discovered. Measurement conditions for proper characterization of the levels by identifying thermal and tunneling processes are discussed in terms of the complexity resulting from the features of self-assembled QDs and multiple paths for electron escape.

Keywords Electron states in low-dimensional structures · Quantum dots · III–V semiconductors · Electrical properties · Deep level transient spectroscopy

Introduction

Deep level transient spectroscopy (DLTS) is a technique for filtering signal transients from the emission of charge carriers at localized band gap energy levels to the conduction or valence band of semiconductors. Performing measurements for varying temperature, the method was developed to transfer data from the time domain into temperature spectra with characteristic features that can be used to identify properties of deep energy levels in semiconductors [1]. When using DLTS to investigate emission properties of charge carriers in quantum dots (QDs), additional problems occur due to the specific properties connected with this kind of structures. Therefore, interpreting DLTS data from self-assembled QDs in the traditional way may give rise to considerable misinterpretations. One reason for this is the varying sizes of QDs, which gives rise to varying properties of most quantities associated with the different elements of the QD ensemble. Another influence on measured results is the possibility of QDs to capture a larger number of electrons, which means that multiparticle statistics must be used to analyse data.

In a series of recent papers, we have demonstrated how such properties can be taken into account and how data can be presented so that the properties of carrier emission from QD structures can be understood [2–6]. This was done by using systems where the QDs are embedded in the depletion region of a Schottky barrier and by measuring the DLTS data as a function of temperature and reverse voltage [5]. Creating graphs as surfaces in a temperature—voltage—DLTS signal space (*TVD*-space) and comparing such data with theory [2–4] gives an opportunity to recognize various paths of charge carrier escape. In the present paper, we demonstrate how the statistics for electron emission from InAs/GaAs QDs is treated in order to understand experimental DLTS-data.

Electron Escape from Quantum Dots and DLTS

DLTS requires the possibility to switch energy levels from positions below to positions above the Fermi-level. This can be achieved by utilizing the possibilities of pushing the

O. Engström (✉)
Microtechnology and Nanoscience, Chalmers University of Technology, 412 96 Goteborg, Sweden
e-mail: olof.engstrom@mc2.chalmers.se

M. Kaniewska
Department of Analysis of Semiconductor Nanostructures, Institute of Electron Technology, Al. Lotników 32/46, 02-668 Warsaw, Poland

depletion region of a Schottky or a p-n diode into thermal non-equilibrium. Figure 1a demonstrates the conduction band of a Schottky diode where QDs are positioned in an n-type semiconductor close to the metal-semiconductor interface. At zero volts applied across the structure, the energy levels of the QDs are found below the Fermi-level of the bulk material. By applying a step voltage in the reverse direction of the diode, the energy levels are raised to positions above the Fermi-level and the electrons captured in the QDs are emitted to the conduction band of the matrix material. This will increase the positive net charge in the depletion region and give rise to a change of the diode capacitance. For a single energy level with a single electron captured and for a pure thermal process, the capacitance transient takes the shape of a decaying exponential function with a time constant equal to $1/e$, where e is the thermal emission rate of electrons from the QDs. This quantity is proportional to a Boltzmann factor with an activation energy determined by the energy needed to release an electron from the QD. Filtering the capacitance transients for different temperatures, for example by box-car or lock-in technique, temperature spectra are obtained with a peak occurring at the temperature where the tuning of the filter coincides with the thermal emission rate e.

An example of DLTS spectra from the QD-samples specified below and investigated in the present work is shown in Fig. 1b. One notices that the curves are considerably influenced by the applied reverse voltage. This originates from a number of properties specific for QDs, which commonly are not found in DLTS measurements on deep level semiconductor impurities. Besides the energy distribution of electron states due to QD size fluctuations, a considerable tunneling contribution exists in combination with multiparticle emission, which gives rise to the metamorphosis among the DLTS curves in Fig. 1b when the voltage is varied. This motivates a more detailed emission statistics for interpreting this kind of data.

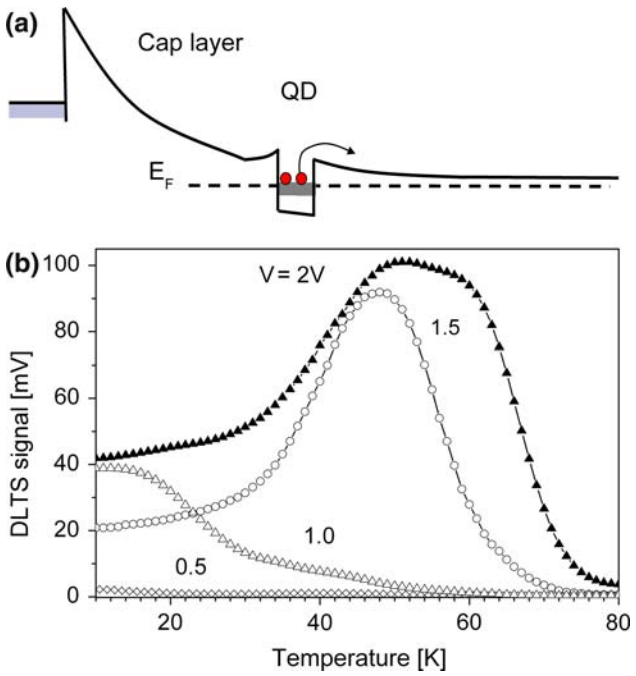

Fig. 1 Conduction band of the Schottky diode during the measurement phase. (**a**) Typical DLTS spectra from InAs/GaAs QD samples taken at different revere bias voltages, V. (**b**) The voltage level of the filling pulse and the emission rate window were fixed at 0 and 543 s^{-1}, respectively

Emission Statistics

The self-assembled InAs/GaAs QDs investigated in this work have a dome-like shape with height/base dimensions in the range of 6/18 nm. This geometry has been found to give rise to two observable electron shells, one with *s*-character at energy distances in the range of 0.11–0.14 eV from the GaAs conduction band edge and a second shell of *p*-character with a corresponding energy interval of 0.08–0.11 eV [5].

Figure 2 shows the energy level scheme with the different escape possibilities marked. Considering the transition paths depicted from left to right in the figure, we notice first the possibility of direct emission from the *s*-level to the conduction band. As will be demonstrated below, in practice, the rate of this step has been found to be surpassed by the two-step emission process from *s* to *p* followed by the transition to the conduction band. An electron captured on the *p*-level can of course be directly transferred to the conduction band by thermal excitation, as well as by tunneling for higher electric fields. This latter mechanism is also possible for the *s*-electrons, and for *s*-electrons thermally excited to the *p*-level. Finally, there is a relaxation process possible from *p* to *s* which needs to be included in a statistical reasoning.

Emission statistics for pure thermal processes, and for a combination of thermal and tunneling processes, has been developed from a starting point where the QDs were assumed to be elements of a grand canonical ensemble [3, 4]. Such a statistics must include the particular properties of the *s*-levels to capture two electrons with an energy level difference smaller than about 4 meV as found by theory in a Hartree-Fock and configuration interaction approximation and from experiment [4]. For the *p*-electrons, only one of four possible states was considered. Here the level splitting is expected to be larger, which limits the *p*-emissions observable by commonly used DLTS set-ups to the state with the deepest energy position.

In Refs. [2] and [3] it was found that the emission rate of electrons from the *s*-shell to the conduction band can be

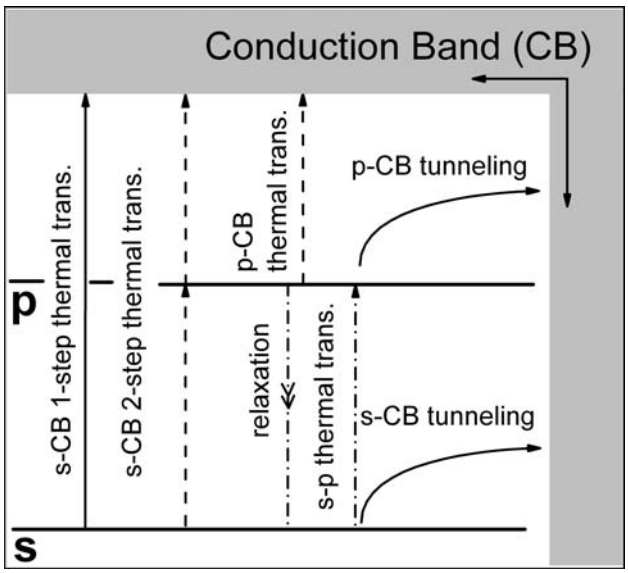

Fig. 2 Energy level scheme and various mechanisms of carrier emission involving the quantum confined energy levels of *s*- and *p*-character

expressed as a combination of the excitation paths shown in Fig. 2 and merged into an "effective" emission rate, $e_{e,r}$

$$e_{e,r} = (c_{s,r} + \Theta_r c_p) X_{s,r} N_c \exp\left(-\frac{\Delta E_s}{kT}\right) + e_{st,r} + e_{pt}\Theta_r \frac{X_p}{X_{s,r}} \exp\left(-\frac{\Delta E_s - \Delta E_p}{kT}\right) \quad (1)$$

where

$$\Theta_r = \left[1 + t_r(e_p + e_{pt})\right]^{-1} \quad (2)$$

and where

$$e_p = c_p N_c X_p \exp\left(-\frac{\Delta E_p}{kT}\right) \quad (3)$$

In Eqs. 1–3 above, $c_{x,r}$ is the electron capture rates, where $x = s, p$ denotes the *s* and *p* transitions and $r = 1, 2$ denotes the number of electrons captured. Further, Θ_r is a "sticking probability" as expressed by Eq. 2 with t_r labelling the time for an electron to relax from the *p*-level to an empty *s*-state. The $X_{x,r}$ factors are the "entropy factors" representing the change in entropy when an electron is emitted. For the present system it has been found that these factors are determined mainly by the electronic degeneracies of the QD system [7]. The quantities $e_{st,r}$ and e_{pt} are the tunneling emission rates from *s*- and *p*-states, respectively, while ΔE_s and ΔE_p are the energy distances from the GaAs conduction band edge to the *s*- and *p*-states, respectively. Finally, *k* is Boltzmann's constant and *T* is absolute temperature.

Figure 3 shows $e_{e,1}$ and e_p as given by Eqs. 1 and 3 in Arrhenius plots assuming Gaussian energy level distributions with standard deviations and other parameter values as presented in Table 1. In Fig. 3a, representing the average level values of the *s* and *p* energy distributions, one notices that the direct transition from the *s*-level to the conduction band occurs only at higher temperatures where the emission rate is too high for most DLTS set-ups. Branches (4) and (3) of the *s* activation curve are broken by a kink when the transition is changed from two-step thermal to two-step thermal/tunneling, respectively. Branches (1) of the *p*-curve and (2) of the *s*-curve represent pure tunneling emission. The vertical position of these latter parts depends on the reverse voltage applied during the DLTS-measurement. Similarly, due to the tunneling from *p* to the conduction band involved in branch (3), the kink point moves with changing reverse voltage. A peak in *TVD*-space occurs when the activation curves intersect the dashed horizontal line representing the rate window for tuning the DLTS filter function. For branches (1) and (2), this means that ridges are created in *TVD*-space when tunneling dominates from *p* and *s*, respectively. For the kink between (3) and (4), it means a dramatic Cape occurring in *TVD*-space when it passes the tuning rate window as will be demonstrated below.

The values along the vertical coordinate in Fig. 3b represent the product between a normalized energy distribution and the emission rate. The two surfaces in the three-dimensional plot, therefore, correspond to the probabilities for emitting an electron from the two energy shells, respectively, at a certain point on the bottom plane. The graphs illustrate the additional complexity involved in the emission process as a result of the varying electron energy eigenvalues, which in turn is a result of varying dot size.

The *TVD*-Space

Plotting DLTS data, *D*, as a function of temperature and voltage defines a space in *T,V,D* coordinates, in which the

Table 1 Data used in calculations for determining quantities presented in Figs. 3–5

Average binding energy, *s*-electrons	125 meV
Standard deviation	13 meV
Average binding energy, *p*-electrons	90 meV
Standard deviation	9 meV
Capture cross sections, *s*-electrons	10^{-13} cm^2
Capture cross sections, *p*-electrons with one electron in *s*-shell	10^{-10} cm^2
Capture cross section, *p*-electron with no electron in *s*-shell	5×10^{-10} cm^2
Time for *p* to *s* electron relaxation (t_r)	10^{-12} s
GaAs doping level in depletion region	1.4×10^{16} cm^{-3}

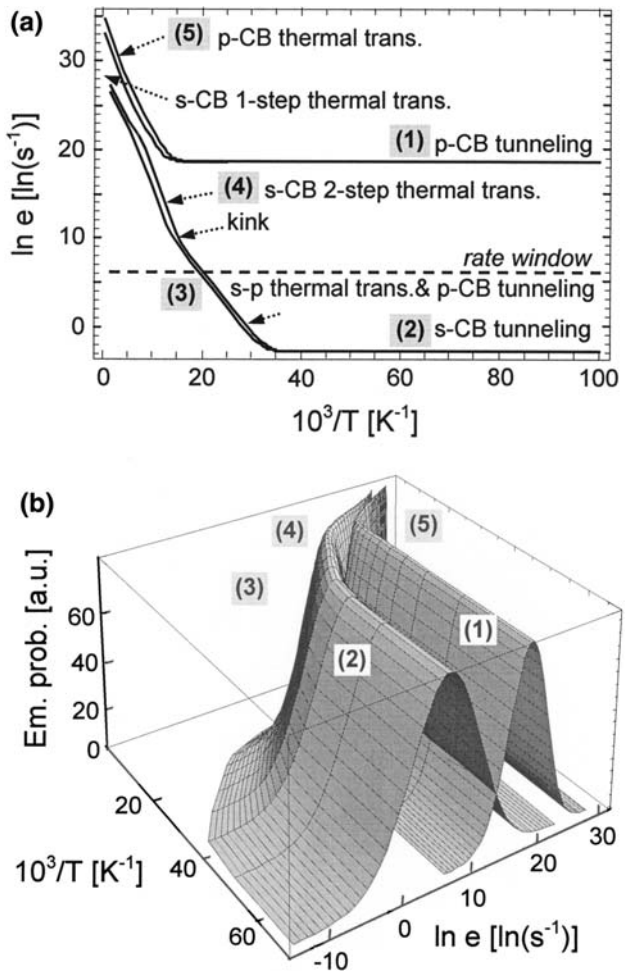

Fig. 3 Arrhenius plot of effective rates of thermal electron emission from the *s*- and *p*-states calculated on the basis of Eqs. 1–3. Parameters used in the calculations are given in Table 1. Numbers relate to regions of the plot in which electron emission is dominated by: (1) tunneling from the *p*-level to the conduction band (CB), (2) tunneling from the *s*-level to CB, (3) combined thermal transition from the *s*-level to the *p*-level and tunneling to CB, (4) two-step thermal transition from the *s*-level to CB via the *p*-level, (5) thermal transition from the *p*-level to CB. The Arrhenius plot calculated in terms of the probability for electron emission from the *s*- and *p*-energy distributions determined by dot size distributions is shown in (**b**)

different emission properties and conditions are revealed in an illustrative way. Figure 4 shows theoretical DLTS spectra presented as contour plots on a *T,V*-plane for an electron trap with two energy levels for captured electrons. In Fig. 4a it is assumed that no tunneling or other dependence on electric field exists. The gradient, grad $D(T,V)$, therefore is zero in the *V*-direction. It should also be mentioned that this representation is highly simplified as no consideration has been taken to the position of the Fermi-level in relation to the energy level distribution. In Fig. 4b the same independence of *V* is assumed, while it is demonstrated how the Fermi-distribution influences the DLTS

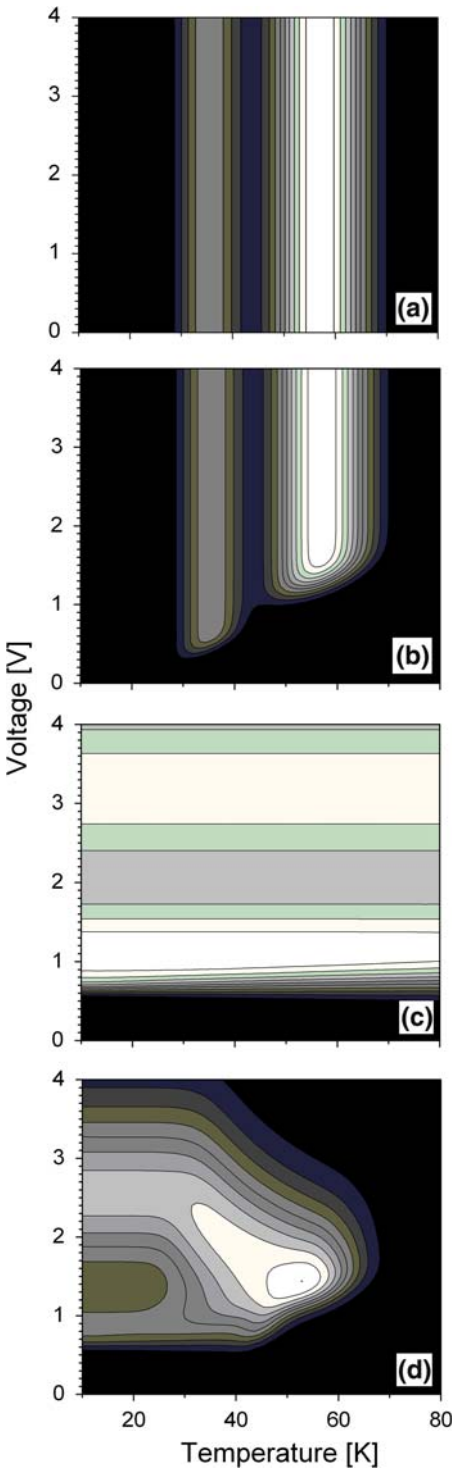

Fig. 4 Contour plots of DLTS signals as a function of temperature and applied sample voltage calculated for different limiting cases: when electrons are thermally activated from two deep energy levels, which are uniformly distributed in the space and the thermal electron emission is not influenced by the electric field effect (**a**), the thermal emission goes from two energy distributed levels localized in space (**b**), when the electron emission from the states is determined by electric field dependent tunneling and thermal processes can be neglected (**c**), properties of plots (**b**) and (**c**) using parameters for QD levels in Table 1 are combined in contour plot (**d**)

characteristic. As can be understood from Fig. 1, a certain voltage is needed in order to bring the energy levels above the Fermi-level and make it possible for electrons to leave the QDs. This is similar to a situation where a trap is localized in space. It influences the *D*-contours and causes gradients in the voltage direction for the lower voltages. A lower slope occurs for the deeper *s* energy levels. The reason is that deeper energy levels occur at a higher temperature, where the Fermi distribution is more smeared out along an energy scale. For a trap level where the only emission possibility would be tunneling, the *TVD*-surface would have a non-zero gradient in the voltage direction only as shown in Fig. 4c. Also in this case the influence of the Fermi distribution is taken into account, which results in the sloping contour lines for the lower voltages. Fig. 4d, finally, is a theoretical contour representation, calculated for the QDs investigated in the present work by using the parameters in Table 1. Here, one notices the horizontal contour lines, and thus vertical gradients, for the lower temperatures, revealing pure tunneling emission in this part of the *TVD*-space. For temperatures above about 30 K, the pattern becomes more complicated because the DLTS signal now is influenced by both thermal and tunneling emission and, for the lower voltages, also by the Fermi-distribution. The influence of the kink, as discussed above in relation to Fig. 3a, occurs as the "Cape" in Fig. 4d at about 60 K and 1.5 V.

In traditional DLTS experiments, the activation energies for particle emission is obtained by measuring multiple temperature spectra for different tuning conditions of the DLTS filter. This requires that the DLTS surface in *TVD*-space has the properties shown in Fig. 4a and b without any gradient contribution in *V* direction. For the surface shown in Fig. 4d, this occurs only at the "Cape".

Experimental Details

The samples subjected to the study contained a single InAs QD plane, which was located 0.4 μm from the Schottky contact and surrounded by barriers made of GaAs. The structures were grown by solid source MBE on (100) oriented highly doped GaAs substrates. GaAs buffer and cap layers were grown at a substrate temperature of 580 °C and were doped with Si to approximately 1.4×10^{16} cm^{-3}. An InAs layer with a nominal thickness of 3 monolayers (MLs) was grown at 510 °C under a repeated sequence, where 0.1 ML depositions included a 2 s growth interruption under an excess of As_2. For DLTS measurements, a DLS-83D system (Semilab, Hungary) equipped with a closed cycle helium cryostat was used. Schottky contacts were fabricated for DLTS investigation by evaporating gold dots of 1 mm diameter through a mechanical mask. AuGeNi ohmic contacts were evaporated on the opposite side of the samples and formed by annealing at 400 °C for 1 min. The leakage current of the prepared Schottky diodes was lower than 10^{-7} A for reverse bias voltages up to 6 V in the temperature range 20–80 K, which was the temperature range used in the experiment. A complementary study was carried out by means of Atomic Force Microscopy (AFM). AFM image and statistical analysis revealed that the uncapped InAs/GaAs QDs with height/base dimensions of about 6/18 nm and density of 3.5×10^{10} cm^{-2} exhibited remarkably low size dispersion on a level of 10% [8].

Experimental Results

In Fig. 5a an experimental *TVD*-surface in a 3D-plot is presented for comparison with the simulated surface shown in Fig. 5b. The fitting procedure was done in the following way. For $T = 13$ K, thermal emission is negligible. For that temperature, the DLTS amplitude was calculated as a function of reverse voltage, by fitting the average electron binding energies of the *s*- and *p*-levels and by using tunneling emission data from Ref. [2]. For the highest temperatures, where thermal emission dominates, the same electron binding energies, given in Table 1, also need to place the "Cape" into the right position by using capture cross sections of the *p*-electrons in the range as obtained by experiments in Ref. [9]. The capture of electrons to the *s*-level was found in Ref. [9] to be much smaller than that for the *p*-level and was set to the value shown in Table 1. This means that emission from the *s*-level only takes place as tunneling or as a two-step transition from *s* to *p* to the conduction band. In order to take into account the influence of the distribution of energy levels, a Gaussian distribution was assumed. The standard deviation of this distribution was fitted into the integration of the functions in the DLTS filtering procedure until the width of the features in the theoretical DLTS surface was in accordance with experiment. The time for *p*- to *s*-relaxation was set to 1 ps as often used in literature data [3]. For increasing values, this quantity did not influence the result until reaching the ns range. We estimate the precision in the determination of average electron binding energies from this method to be within the range of the Gaussian standard deviation.

A number of features recognized from Fig. 5b and discussed in relation to Fig. 4 can be observed. The tunneling ridges originated from *s*- and *p*-electrons are noticed at the lower temperatures, separated by the "Tunneling Lake", which is the minimum signal originating from tunnel emissions between the two distributions of *s*- and *p*-levels. For the higher temperatures, the two-step thermal emission can be identified as the "Thermal Slope" at the lower

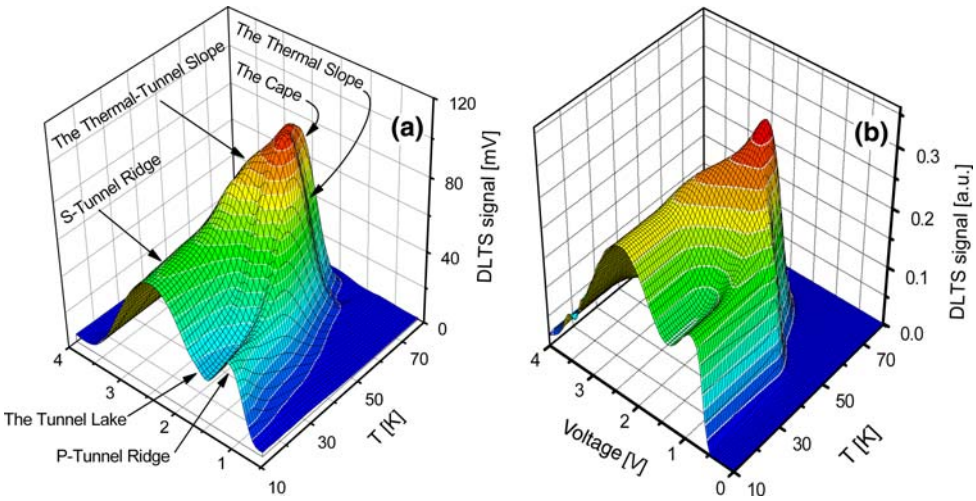

Fig. 5 Comparison of experimental (**a**) and theoretical (**b**) DLTS spectra in *TVD*-space for the InAs/GaAs quantum dot samples calculated for QD data from Table 1. The measurement was performed with the voltage level of the filling pulses and the emission rate window equal to 0 and 543 s^{-1}, respectively

voltages, turning into the "Thermal-Tunneling Slope" at about $V = 2$ V on the farther side of the "Cape". The theoretical correspondence, calculated by including the parameter values of Table 1, shows all the features pointed out in Fig. 5a, even if certain differences are observed in some details. However, the theoretical graph in Fig. 5b in combination with the theoretical activation plots in Fig. 3 serve the purpose of identifying the features of the experimental data.

Due to the overlap of the *s* and *p* energy distribution, pure separation of influences from the two electron shells can be done only at the lowest temperatures and the highest and the lowest voltages. This is important to be taken into consideration in tunneling transient spectroscopy, which has been proposed and used at a low temperature to probe the pure tunneling from the self-assembled InAs/GaAs QDs [10, 11]. The most serious problem results from the QD size fluctuation effect and the related width of the energy level distributions. In spite of using Gaussian fitting procedure, it makes basic difficulties in positioning signals in DLTS spectra and also in differing between the *p*- and *s*-states. As noticed in Fig. 3b, a deeper energy part of the *p*-state distribution and a lower energy part of the *s*-state distribution both contributes to the DLTS signal at the same rate window. As shown in Ref. [6], this causes an illusory anomaly in the dependence of *p*-DLTS tunneling signals on the electric field. In order to separate *p*- and *s*-influence along the temperature direction, one may either follow the "Cape" [12] and thus lock the measurement to the kink point in Fig. 3a or use special voltage pulse schemes [13].

Conclusions

We have demonstrated that the main electronic properties of QDs can be revealed and understood by plotting experimental DLTS spectra in a *TVD*-space and comparing with theory obtained from a statistical analysis. The resulting 3D/contour graphs compile tunneling and thermal processes involved in the two-level system presented. For a rigorous characterization of QD-related electron states by DLTS, measurement conditions need to be chosen such that data are collected in directions on the *TV*-plane where contour DLTS lines are either horizontal or vertical. However, due to overlapping energy distributions and mixed emission mechanisms, standard DLTS methodology [1] becomes less straightforward for finding parameters of confined QD energy states. Therefore, in order to extract QD data as presented in Table 1, fitting theory to experimental *TVD* surfaces gives the most reliable results.

Acknowledgements This work was supported by the Chalmers MC2SOI project, by the Polish Min. of Science and Higher Education (project no. 3T11B00729 and 1.12.053) and by the European Seventh Framework Program through the Network of Excellence NANOSIL.

References

1. D.V. Lang, J. Appl. Phys. **45**, 3023 (1974)
2. Y. Fu, O. Engström, Y. Luo, J. Appl. Phys. **96**, 6477 (2004)
3. O. Engström, P.T. Landsberg, Phys. Rev. B **72**, 075360 (2005)
4. O. Engström, P.T. Landsberg, Y. Fu, Mater. Sci. Eng. C **26**, 739 (2006)
5. O. Engström, M. Kaniewska, W. Jung, M. Kaczmarczyk, Appl. Phys. Lett. **91**, 33110 (2007)
6. O. Engström, M. Kaniewska, M. Kaczmarczyk, W. Jung, Appl. Phys. Lett. **91**, 133117 (2007)
7. O. Engström, Y. Fu, A. Eghtedari, Physica E **27**, 380 (2005)
8. M. Kaczmarczyk, O. Engström, M. Kaniewska, B. Surma, 9-th Workshop on Expert Evaluation & Control of Compound Semiconductor Materiale & Technologies (Exmatec), June 1–4, 2008, Lodz, Poland, to be presented
9. O. Engström, M. Kaniewska, Y. Fu, J. Piscator, M. Malmkvist, Appl. Phys. Lett. **85**, 2908 (2004)

10. S. Schultz, A. Schramm, C. Heyn, W. Hansen, Phys. Rev. B **74**, 33311 (2006)
11. E. Geller, E. Stock, C. Kapteyn, R.L. Sellin, D. Bimberg, Phys. Rev. B **73**, 205331 (2006)
12. M. Kaniewska, O. Engström, M. Kaczmarczyk, B. Surma, W. Jung, G. Zaremba, to be published in Phys. Stat. Sol. (c)
13. O. Engström, M. Malmkvist, Y. Fu, H.Ö. Olafsson, E.Ö. Sveinbjörnsson, Appl. Phys. Lett. **83**, 3578 (2003)